A ROBUST DISCRETIZATION OF THE REISSNER–MINDLIN PLATE WITH ARBITRARY POLYNOMIAL DEGREE[*]

Dietmar Gallistl

Friedrich-Schiller-Universität Jena, 07737 Jena, Germany
Email: dietmar.gallistl@uni-jena.de

Mira Schedensack

Universität Leipzig, PF 10 09 20, 04009 Leipzig, Germany
Email: mira.schedensack@math.uni-leipzig.de

Abstract

A numerical scheme for the Reissner–Mindlin plate model is proposed. The method is based on a discrete Helmholtz decomposition and can be viewed as a generalization of the nonconforming finite element scheme of Arnold and Falk [SIAM J. Numer. Anal., 26(6):1276–1290, 1989]. The two unknowns in the discrete formulation are the in-plane rotations and the gradient of the vertical displacement. The decomposition of the discrete shear variable leads to equivalence with the usual Stokes system with penalty term plus two Poisson equations and the proposed method is equivalent to a stabilized discretization of the Stokes system that generalizes the Mini element. The method is proved to satisfy a best-approximation result which is robust with respect to the thickness parameter t.

Mathematics subject classification: 65N10, 65N15, 73K10, 73K25.
Key words: Reissner–Mindlin plate, Nonconforming finite element, Discrete Helmholtz decomposition, Robustness.

1. Introduction

The transverse displacement w of a thin elastic plate of thickness $t > 0$ whose mid-surface is a bounded, open, simply connected, polygonal Lipschitz domain $\Omega \subseteq \mathbb{R}^2$ and the rotation ϕ of the plate's fibers normal to the mid-surface are described by the Reissner–Mindlin plate model. Given a (re-scaled) transverse load $f \in L^2(\Omega)$, the Reissner–Mindlin plate problem with clamped boundary condition seeks $w \in H_0^1(\Omega)$ and $\phi \in \Phi := [H_0^1(\Omega)]^2$ such that

$$a(\phi, \psi) + \lambda t^{-2}(\nabla w - \phi, \nabla v - \psi)_{L^2(\Omega)} = (f, v)_{L^2(\Omega)} \quad \text{for all } (v, \psi) \in H_0^1(\Omega) \times \Phi. \qquad (1.1)$$

Here, the bilinear form $a(\cdot, \cdot)$ is defined by $a(\phi, \psi) := (\varepsilon(\phi), \mathbb{C}\varepsilon(\psi))_{L^2(\Omega)}$ for the linear green strain $\varepsilon(\cdot) = \operatorname{sym} D(\cdot)$ and the linear elasticity tensor $\mathbb{C}$ that acts on any symmetric matrix $A \in \mathbb{R}^{2 \times 2}$ as follows

$$\mathbb{C}A = \frac{E}{12(1 - \nu^2)}((1 - \nu)A + \nu \operatorname{tr}(A)I_{2 \times 2}).$$

For isotropic materials it is determined by Young's modulus $E > 0$ and the Poisson ratio $0 < \nu < 1/2$. Those also determine the constant λ in (1.1), which reads $\lambda = (1 + \nu)^{-1}E\kappa/2$ with a shear correction factor κ usually chosen as $5/6$. More details on the mathematical model can be found in [5,6].

Standard schemes are known to exhibit *shear locking* and yield poor results for small thickness $t \ll h$. The reader is referred to [6,9] and the references therein for an overview of numerical schemes. It was the observation of Brezzi and Fortin [8] that the Helmholtz decomposition of the shear variable $\zeta := t^{-2}(\nabla w - \phi)$ may serve as the key for the robust numerical approximation of (1.1). Arnold and Falk [3] discovered a discrete analogue to that decomposition which led to a robust nonconforming finite element discretisation. Their discrete Helmholtz decomposition turned out useful for other purposes, too; but in its original form it is restricted to piecewise affine finite element functions and so to the lowest-order case. In [13] the generalization of the discrete Helmholtz decomposition to higher polynomial degrees from [14] was combined with the Taylor–Hood element [5] and optimal-order convergence rates were proved for the rotation variable through a superconvergence analysis. In this article we present and analyze the generalization of Arnold and Falk's scheme to higher polynomial degrees. This involves higher-order analogues of the Mini element. We formulate the new scheme in §2 and give robust a priori error estimates in §3. The numerical experiments of §4 investigate the performance of the method.

Standard notation on Lebesgue and Sobolev spaces applies throughout this paper. The L^2 inner product is denoted by $(v, w)_{L^2(\Omega)}$. The space of $L^2(\Omega)$ functions with vanishing global average reads $L^2_0(\Omega)$. For a function v and a vector field ψ, the following differential operators are defined

$$\operatorname{div} \psi = \partial_1 \psi_1 + \partial_2 \psi_2, \quad \operatorname{rot} \psi = \partial_1 \psi_2 - \partial_2 \psi_1, \quad \operatorname{Curl} v = \begin{pmatrix} -\partial_2 v \\ \partial_1 v \end{pmatrix}.$$

The notation $A \lesssim B$ abbreviates $A \leq CB$ for some constant C that is independent of the mesh size and the plate's thickness t.

2. The Method

This section is devoted to the precise definition of the novel method in Section 2.1. The discretization space for ϕ is stabilized with local bubble functions. Those can be condensated in the resulting system matrix. This is explained in more detail in Section 2.2.

2.1. Definition of the method

The new numerical scheme for Reissner–Mindlin plates is based on an equivalent reformulation of the original problem (1.1) based on the space of gradients $Z := \nabla H^1_0(\Omega)$. We assume that Ω is simply connected. With the spaces $X := [L^2(\Omega)]^2$ and $Q := H^1(\Omega) \cap L^2_0(\Omega)$, the Helmholtz decomposition gives the following characterization

$$Z = \{\sigma \in X \mid (\sigma, \operatorname{Curl} q)_{L^2(\Omega)} = 0 \text{ for all } q \in Q\}.$$

Note that, in two dimensions, the Curl operator is only the rotated gradient and therefore $H^1(\Omega)$ equals the space of all $L^2(\Omega)$ functions whose Curl is in $L^2(\Omega)$. Let $\eta \in H(\operatorname{div}, \Omega)$ be given with $-\operatorname{div} \eta = f$. The integration by parts and the substitutions $\sigma := \nabla w$ and $\tau := \nabla v$ show that (1.1) is equivalent to finding $\sigma \in Z$ and $\phi \in \Phi$ such that

$$a(\phi, \psi) + \lambda t^{-2}(\phi - \sigma, \psi - \tau)_{L^2(\Omega)} = (\eta, \tau)_{L^2(\Omega)} \quad \text{for all } (\tau, \psi) \in Z \times \Phi. \tag{2.1}$$

While on the continuous level this is merely a reformulation of (1.1), discretizations based on (2.1) turn out to benefit from an intrinsic discrete Helmholtz decomposition.

Let $\mathcal{T}$ denote a regular triangulation of Ω. For any $T \in \mathcal{T}$ let h_T denote its diameter and let $P_k(T)$ denote the polynomial functions over T of degree not larger than $k \geq 0$. The piecewise polynomial functions with respect to $\mathcal{T}$ are denoted by $P_k(\mathcal{T})$ and the space of vector fields whose components belong to $P_k(\mathcal{T})$ reads $P_k(\mathcal{T}; \mathbb{R}^2)$. The L^2 projection onto (any power of) $P_k(\mathcal{T})$ is denoted by Π_k. The following notation is employed for subspaces of continuous functions

$$S^k(\mathcal{T}) := P_k(\mathcal{T}) \cap H^1(\Omega) \quad \text{and} \quad S_0^k(\mathcal{T}) := P_k(\mathcal{T}) \cap H_0^1(\Omega)$$

with the vector-valued versions $S^k(\mathcal{T}; \mathbb{R}^2)$ and $S_0^k(\mathcal{T}; \mathbb{R}^2)$.

Let $k \geq 0$ be a nonnegative integer and $\ell \in \mathbb{N}$ and define the space of bubble functions related to k as

$$\mathcal{B}(\mathcal{T}; k) := \left\{ b_h \in L^2(\Omega) \;\middle|\; \begin{array}{l} \forall T \in \mathcal{T} \, \exists v_{T,k} \in P_k(T) \text{ with} \\ b_h|_T = (\lambda_1 \lambda_2 \lambda_3)^\ell \, v_{T,k} \end{array} \right\}$$

with $\lambda_1, \lambda_2, \lambda_3$ the barycentric coordinates on T. The functions from $\mathcal{B}(\mathcal{T}; k)$ serve as (purely local) stabilization of the numerical scheme to guarantee a discrete inf-sup condition, see §3. There are two relevant choices for the parameter ℓ, namely

$$\ell = 1 \quad \text{or} \quad \ell = \lceil (k+2)/3 \rceil \tag{2.2}$$

with $\lceil s \rceil$ the smallest integer not smaller than s. This will be commented on in §2.2.1 and in Remark 3.2. Define the spaces

$$\Phi_h := [S_0^{k+1}(\mathcal{T}) + \mathcal{B}(\mathcal{T}; k)]^2, \quad X_h := P_k(\mathcal{T}; \mathbb{R}^2), \quad Q_h := S^{k+1}(\mathcal{T}) \cap L_0^2(\Omega).$$

The space of discrete gradients reads

$$Z_h := \{ \sigma_h \in X_h \mid (\sigma_h, \operatorname{Curl} q_h)_{L^2(\Omega)} = 0 \text{ for all } q_h \in Q_h \}. \tag{2.3}$$

Note that $Z_h \not\subseteq Z$ in general. The discretization of (2.1) seeks $(\sigma_h, \phi_h) \in Z_h \times \Phi_h$ such that for all $(\tau_h, \psi_h) \in Z_h \times \Phi_h$ there holds

$$a(\phi_h, \psi_h) + \lambda t^{-2} (\Pi_k \phi_h - \sigma_h, \Pi_k \psi_h - \tau_h)_{L^2(\Omega)} = (\eta, \tau_h)_{L^2(\Omega)}. \tag{2.4}$$

Here, the L^2 projection Π_k plays the role of a reduction or reduced integration operator. Such operators are commonly met in the discretization of Reissner–Mindlin plates [6].

Remark 2.1. In the lowest-order case, $k = 0$, the method (2.4) coincides with the scheme proposed by [3] (possibly up to the right-hand side). The discrete Helmholtz decomposition by [3] shows that in this case the space Z_h equals the space of piecewise gradients of the nonconforming P_1 finite element functions [12].

2.2. Computational aspects

This subsection describes how to practically implement the discrete scheme (2.4). In particular, it is shown that after static condensation the resulting system is of moderate size.

2.2.1. Choice of the stabilization

For $\ell < \lceil (k+2)/3 \rceil$, the spaces $S_0^{k+1}(\mathcal{T})$ and $\mathcal{B}(\mathcal{T}; k)$ have a nontrivial intersection and therefore do not form a direct sum in the definition of Φ_h. This may cause difficulties in the design of

local shape functions of Φ_h. For $\ell = 1$, all basis functions corresponding to interior degrees of freedom are already contained in $\mathcal{B}(\mathcal{T}; k)$ and, hence, a basis can be defined by simply dropping those basis functions from $S_0^{k+1}(\mathcal{T})$. The choice $\ell \geq \lceil (k+2)/3 \rceil$ circumvents this technicality by allowing a direct sum of the Lagrange finite element space and the stabilization.

2.2.2. Static condensation

The constraint for the space $Z_h \subseteq X_h$ is incorporated via a Lagrange multiplier $\alpha_h \in Q_h$. Then, system (2.4) may be reformulated as seeking $(\sigma_h, \phi_h, \alpha_h) \in X_h \times \Phi_h \times Q_h$ such that, for all $(\tau_h, \psi_h, \beta_h) \in X_h \times \Phi_h \times Q_h$

$$a(\phi_h, \psi_h) + \lambda t^{-2}(\Pi_k \phi_h - \sigma_h, \Pi_k \psi_h - \tau_h)_{L^2(\Omega)} + (\tau_h, \operatorname{Curl} \alpha_h)_{L^2(\Omega)} = (\eta, \tau_h)_{L^2(\Omega)}$$
$$(\sigma_h, \operatorname{Curl} \beta_h)_{L^2(\Omega)} = 0.$$

The condition that the average of α over Ω vanishes can be included in the system by another (one-dimensional) Lagrange multiplier. However, as this does not affect the condensation described below, we will neglect this in the following for the ease of presentation. If one identifies ϕ_h, σ_h, α_h with their coefficient vectors with respect to a basis of Φ_h, X_h, Q_h, the above system reads

$$\begin{bmatrix} \mathbf{A} + \lambda t^{-2}\mathbf{M} & -\lambda t^{-2}\mathbf{B} & 0 \\ -\lambda t^{-2}\mathbf{B}^* & \lambda t^{-2}\mathbf{D} & \mathbf{C} \\ 0 & \mathbf{C}^* & 0 \end{bmatrix} \begin{bmatrix} \phi_h \\ \sigma_h \\ \alpha_h \end{bmatrix} = \begin{bmatrix} 0 \\ \mathbf{g} \\ 0 \end{bmatrix}$$

for the stiffness matrix $\mathbf{A}$ and the reduced mass matrix $\mathbf{M}$ with respect to Φ_h, the matrix $\mathbf{B}$ representing the bilinear form $(\Pi_k \psi_h, \tau_h)_{L^2(\Omega)}$, the matrix $\mathbf{C}$ representing $(\tau_h, \operatorname{Curl} \beta_h)_{L^2(\Omega)}$, the mass matrix $\mathbf{D}$ with respect to X_h, and the load vector $\mathbf{g}$. In a first step, the variable σ_h is eliminated from the system. The matrix $\mathbf{D}$ is block diagonal and can thus be inverted explicitly. The equations of the Schur complement read

$$\begin{bmatrix} \mathbf{A} & \mathbf{B}\mathbf{D}^{-1}\mathbf{C} \\ \mathbf{C}^*\mathbf{D}^{-1}\mathbf{B}^* & -\lambda^{-1}t^2\mathbf{C}^*\mathbf{D}^{-1}\mathbf{C} \end{bmatrix} \begin{bmatrix} \phi_h \\ \alpha_h \end{bmatrix} = \begin{bmatrix} \mathbf{B}\mathbf{D}^{-1}\mathbf{g} \\ -\lambda^{-1}t^2\mathbf{C}^*\mathbf{D}^{-1}\mathbf{g} \end{bmatrix}.$$

In a second step, the component of ϕ_h that belongs to the space $\mathcal{B}(\mathcal{T}; k)$ is eliminated. As it merely represents a local stabilization, this component is of marginal interest for the approximation of ϕ, but it may be required for reconstructing σ_h in a post-processing step. The components of ϕ_h are separated so that we write $\phi_h = (\phi_h^k; \phi_h^b)$ for ϕ_h^k the coefficients of the P_k interpolation of ϕ_h^k and ϕ_h^b the coefficients describing the bubble part. It should be noted that for practical reasons the bubble functions may be modified such that they are consistent with the interior degrees of freedom of the standard Lagrange elements. This does not change the space Φ_h but is nevertheless useful if one wants to enforce that ϕ_h^k equals the P_k finite element interpolation of ϕ_h. The stiffness matrix $\mathbf{A}$ and the matrix $\mathbf{B}$ are then organized blockwise as follows

$$\mathbf{A} = \begin{bmatrix} \mathbf{A}_{kk} & \mathbf{A}_{kb} \\ \mathbf{A}_{kb}^* & \mathbf{A}_{bb} \end{bmatrix} \quad \text{and} \quad \mathbf{B} = \begin{bmatrix} \mathbf{B}_k \\ \mathbf{B}_b \end{bmatrix}.$$

The bubble part $\mathbf{A}_{bb}$ is block-diagonal and can be inverted explicitly. The resulting condensed system reads

$$
\begin{bmatrix}
\mathbf{A}_{kk} - \mathbf{A}_{kb}\mathbf{A}_{bb}^{-1}\mathbf{A}_{kb}^* & (\mathbf{B}_k - \mathbf{A}_{kb}\mathbf{A}_{bb}^{-1}\mathbf{B}_b)\mathbf{D}^{-1}\mathbf{C} \\
\mathbf{C}^*\mathbf{D}^{-1}(\mathbf{B}_k^* - \mathbf{B}_b^*\mathbf{A}_{bb}^{-1}\mathbf{A}_{kb}^*) & -\mathbf{C}^*\mathbf{D}^{-1}(\lambda^{-1}t^2\mathbf{I} + \mathbf{B}_b^*\mathbf{A}_{bb}^{-1}\mathbf{B}_b\mathbf{D}^{-1})\mathbf{C}
\end{bmatrix}
\begin{bmatrix}
\phi_h^k \\
\alpha_h
\end{bmatrix}
$$
$$
= \begin{bmatrix}
(\mathbf{B}_k - \mathbf{A}_{kb}\mathbf{A}_{bb}^{-1}\mathbf{B}_b)\mathbf{D}^{-1}\mathbf{g} \\
-\mathbf{C}^*\mathbf{D}^{-1}(\lambda^{-1}t^2\mathbf{I} + \mathbf{B}_b^*\mathbf{A}_{bb}^{-1}\mathbf{B}_b\mathbf{D}^{-1})\mathbf{g}
\end{bmatrix}.
$$

This is the system that needs to be solved. The remaining components ϕ_h^b and σ_h are then reconstructed from the foregoing relations (if required).

The number of unknowns in this system, hence, is $\dim(S_0^{k+1}(\Omega;\mathbb{R}^2)) + \dim(Q_h)$. Up to degrees of freedom on the boundary, this is the dimension of a standard scheme for approximating (1.1).

3. Numerical Analysis of the Scheme

This section proves in a first step a discrete inf-sup condition for the pairing (Φ_h, Q_h). This pair generalizes the Mini finite element [2] to higher polynomial degrees. Based on this result and the equivalence of (2.4) to the mixed system from Lemma 3.2 below, the error estimate is proved in Theorem 3.1.

Lemma 3.1 (discrete inf-sup condition). *There exists a constant $C < \infty$ such that any $q_h \in Q_h$ satisfies*

$$
\|q_h\|_{L^2(\Omega)} \leq C \sup_{\psi_h \in \Phi_h \setminus \{0\}} \frac{(\psi_h, \operatorname{Curl} q_h)_{L^2(\Omega)}}{\|\nabla \psi_h\|_{L^2(\Omega)}}.
$$

Proof. The proof follows in three steps.

Step 1. Let $T \in \mathcal{T}$ be fixed. Let $N \in \mathbb{N}$ denote the dimension of $P_k(T)$ and let $(\psi_{T,j})_{j\in\{1,\ldots,N\}}$ denote a basis of $P_k(T)$. In a preliminary step, we construct a basis $\varphi_{T,j}$ of the bubble space $\mathcal{B}(\{T\}, k)$ such that $(\varphi_{T,j}, \psi_{T,m})_{L^2(T)} = \delta_{jm}$ for all $j, m \in \{1, \ldots, N\}$. Here and in the following, δ_{jm} denotes the Kronecker symbol.

Define the matrix $M \in \mathbb{R}^{N\times N}$ by

$$
M_{mn} := \big(\psi_{T,m}, (\lambda_1\lambda_2\lambda_3)^\ell \psi_{T,n}\big)_{L^2(T)} \qquad \text{for all } m, n \in \{1, \ldots, N\}
$$

with ℓ from the definition of $\mathcal{B}(\mathcal{T}; k)$ and the barycentric coordinates $\lambda_1, \lambda_2, \lambda_3$ of T. Note that the matrix M is positive definite and thus regular. Let $\beta_j := M^{-1}e_j \in \mathbb{R}^N$ with the unit vector e_j, i.e., $e_{j,m} = \delta_{jm}$. Note that β_j only depends on the area of T, and its Euclidean norm satisfies the scaling $|\beta_j| \lesssim h_T^{-2}$. Define

$$
\varphi_{T,j} := \sum_{n=1}^N \beta_{j,n}(\lambda_1\lambda_2\lambda_3)^\ell \psi_{T,n}.
$$

Then, the definition of $\varphi_{T,j}$ and the scaling of β_j and the basis functions imply

$$
(\varphi_{T,j}, \psi_{T,m})_{L^2(T)} = e_m \cdot (M\beta_j) = \delta_{jm}, \tag{3.1a}
$$
$$
\|\nabla\varphi_{T,j}\|_{L^2(T)} \lesssim h_T^{-2}. \tag{3.1b}
$$

Step 2. Let $I : \Phi \to S_0^1(\mathcal{T}; \mathbb{R}^2)$ be a quasi-interpolation operator with (local) approximation and stability properties [6, 11]

$$\|h_T^{-1}(v - Iv)\|_{L^2(T)} + \|\nabla Iv\|_{L^2(T)} \lesssim \|\nabla v\|_{L^2(\omega_T)} \quad \text{for any } T \in \mathcal{T}$$

where $\omega_T := \cup\{K \in \mathcal{T} \mid K \cap T \neq \emptyset\}$. Given $q_h \in Q_h$, the continuous inf-sup condition of the divergence operator [1, 6, 7] and the change of coordinates $(x_1, x_2) \mapsto (-x_2, x_1)$ guarantees the existence of $v \in H_0^1(\Omega; \mathbb{R}^2)$ with $\|\nabla v\|_{L^2(\Omega)} = 1$ and

$$\|q_h\|_{L^2(\Omega)} \lesssim -(q_h, \operatorname{rot} v)_{L^2(\Omega)} = (\operatorname{Curl} q_h, v)_{L^2(\Omega)}.$$

In what follows, the superscript (ν) for $\nu \in \{1, 2\}$ refers to the component of a vector field. The vector-valued version of the scalar-valued basis $(\psi_{T,j})_{j=1}^N$ then reads $(\psi_{T,j}^{(\nu)})_{j=1,\dots,N}^{\nu=1,2}$ with $\psi_{T,j}^{(\nu)} = \psi_{T,j} e_\nu$ and analogous notation for $\varphi_{T,j}^{(\nu)}$. Define coefficients $\alpha_{T,j}^{(\nu)} \in \mathbb{R}$ for $j = 1, \dots, N$ and $\nu = 1, 2$ by

$$\alpha_{T,j}^{(\nu)} := (v - Iv, \psi_{T,j}^{(\nu)})_{L^2(T)}$$

and set

$$v_h := Iv + \sum_{T \in \mathcal{T}} \sum_{j=1}^N \sum_{\nu=1}^2 \alpha_{T,j}^{(\nu)} \varphi_{T,j}^{(\nu)} \in \Phi_h.$$

Since $\operatorname{Curl} q_h \in P_k(\mathcal{T}; \mathbb{R}^2)$ is a polynomial of degree $\leq k$, there exist coefficients $a_{T,j}^{(\nu)}$ with

$$\operatorname{Curl} q_h = \sum_{T \in \mathcal{T}} \sum_{j=1}^N \sum_{\nu=1}^2 a_{T,j}^{(\nu)} \psi_{T,j}^{(\nu)}.$$

The definitions of the basis functions $\varphi_{T,j}^{(\nu)}$ and of $\alpha_{T,j}^{(\nu)}$ imply for all $T \in \mathcal{T}$

$$\sum_{j=1}^N \sum_{\nu=1}^2 \alpha_{T,j}^{(\nu)} (\varphi_{T,j}^{(\nu)}, \operatorname{Curl} q_h)_{L^2(\Omega)} = \sum_{j=1}^N \sum_{\nu=1}^2 \alpha_{T,j}^{(\nu)} a_{T,j}^{(\nu)}$$

$$= \sum_{j=1}^N \sum_{\nu=1}^2 a_{T,j}^{(\nu)} (v - Iv, \psi_{T,j}^{(\nu)})_{L^2(\Omega)} = (v - Iv, \operatorname{Curl} q_h)_{L^2(T)}.$$

The definition of v_h therefore implies

$$(v_h, \operatorname{Curl} q_h)_{L^2(\Omega)}$$

$$= (Iv, \operatorname{Curl} q_h)_{L^2(\Omega)} + \sum_{T \in \mathcal{T}} \sum_{j=1}^N \sum_{\nu=1}^2 \alpha_{T,j}^{(\nu)} (\varphi_{T,j}^{(\nu)}, \operatorname{Curl} q_h)_{L^2(\Omega)}$$

$$= (v, \operatorname{Curl} q_h)_{L^2(\Omega)}. \tag{3.2}$$

Step 3. This step bounds $\|\nabla v_h\|_{L^2(\Omega)}$. The triangle inequality and the stability of the quasi-interpolation I prove

$$\|\nabla v_h\|_{L^2(\Omega)} \lesssim \|\nabla v\|_{L^2(\Omega)} + \left(\sum_{T \in \mathcal{T}} \sum_{j=1}^N \sum_{\nu=1}^2 |\alpha_{T,j}^{(\nu)}|^2 \, \|\nabla \varphi_{T,j}\|_{L^2(T)}^2 \right)^{1/2}.$$

The definition of $\alpha_{T,j}^{(\nu)}$, the Cauchy inequality, the scaling properties of the basis functions $\psi_{T,j}$ and the approximation properties of I show

$$|\alpha_{T,j}^{(\nu)}| \leq \|h_T^{-1}(v - Iv)\|_{L^2(T)}\|h_T\psi_{T,j}\|_{L^2(T)} \leq \|\nabla v\|_{L^2(\omega_T)}h_T^2.$$

On the other hand, (3.1) proves $\|\nabla\varphi_{T,j}\|_{L^2(\Omega)} \lesssim h_T^{-2}$. Note that the support of $\varphi_{T,j}$ is T. The finite overlap of the patches ω_T and the combination of the above inequalities leads to

$$\|\nabla v_h\|_{L^2(\Omega)} \lesssim \|\nabla v\|_{L^2(\Omega)}.$$

This concludes the proof. □

Remark 3.1. For $k \geq 3$, the basis functions of $S_k(T)$ have interior degrees of freedom. Therefore they can compensate some moments of $\operatorname{Curl} q_h$ in (3.2) and the choice $\ell = \lceil (k+2)/3 \rceil$ may bear some redundancies in that it would be possible to remove some of the functions in $\mathcal{B}(\mathcal{T};k)$. However, §2.2.2 shows that those bubble functions can be eliminated by building the Schur complement. Therefore, the number of bubble functions does not influence the size of the system that has to be solved and, thus, the additional number of bubble functions in the method can be accepted.

Remark 3.2. Note that for the discrete inf-sup condition, it suffices to consider the smaller space $[S_0^1(\mathcal{T}) + \mathcal{B}(\mathcal{T};k)]^2$ instead of Φ_h and even the choice of any $\ell \geq 1$ would be possible. The spaces Φ_h and Q_h chosen here are balanced with respect to their approximation properties.

The numerical analysis of the discretization (2.4) relies on the equivalence with a mixed system. This equivalence is based on a discrete Helmholtz decomposition and is proved in Lemma 3.2 below. The continuous analogue was proved in [8]. The equivalent mixed system seeks $(\varrho, \phi, p, \sigma) \in Z \times \Phi \times Q \times Z$ such that, for all $(\xi, \psi, q, \tau) \in Z \times \Phi \times Q \times Z$,

$$(\varrho, \xi)_{L^2(\Omega)} = (\eta, \xi)_{L^2(\Omega)}, \tag{3.3a}$$

$$a(\phi, \psi) - (\psi, \operatorname{Curl} p)_{L^2(\Omega)} - (\varrho, \psi)_{L^2(\Omega)} = 0, \tag{3.3b}$$

$$-(\phi, \operatorname{Curl} q)_{L^2(\Omega)} - \lambda^{-1}t^2(\operatorname{Curl} p, \operatorname{Curl} q)_{L^2(\Omega)} = 0, \tag{3.3c}$$

$$(\sigma, \tau)_{L^2(\Omega)} - (\phi, \tau)_{L^2(\Omega)} = \lambda^{-1}t^2(\eta, \tau)_{L^2(\Omega)}. \tag{3.3d}$$

The discrete mixed system seeks $(\varrho_h, \phi_h, p_h, \sigma_h) \in Z_h \times \Phi_h \times Q_h \times Z_h$ such that, for all $(\xi_h, \psi_h, q_h, \tau_h) \in Z_h \times \Phi_h \times Q_h \times Z_h$,

$$(\varrho_h, \xi_h)_{L^2(\Omega)} = (\eta, \xi_h)_{L^2(\Omega)}, \tag{3.4a}$$

$$a(\phi_h, \psi_h) - (\psi_h, \operatorname{Curl} p_h)_{L^2(\Omega)} - (\varrho_h, \psi_h)_{L^2(\Omega)} = 0, \tag{3.4b}$$

$$-(\phi_h, \operatorname{Curl} q_h)_{L^2(\Omega)} - \lambda^{-1}t^2(\operatorname{Curl} p_h, \operatorname{Curl} q_h)_{L^2(\Omega)} = 0, \tag{3.4c}$$

$$(\sigma_h, \tau_h)_{L^2(\Omega)} - (\phi_h, \tau_h)_{L^2(\Omega)} = \lambda^{-1}t^2(\eta, \tau_h)_{L^2(\Omega)}. \tag{3.4d}$$

For $k = 0$, the equivalence with (2.4) was observed by [3], see also Remark 2.1. The following result holds for any $k \geq 0$.

Lemma 3.2 (equivalent system). *If $(\sigma_h, \phi_h) \in Z_h \times \Phi_h$ is a solution of (2.4), then there exists $(\varrho_h, p_h) \in Z_h \times Q_h$ such that $(\varrho_h, \phi_h, p_h, \sigma_h)$ solves (3.4). On the other hand, if $(\varrho_h, \phi_h, p_h, \sigma_h) \in Z_h \times \Phi_h \times Q_h \times Z_h$ is a solution of (3.4), then (σ_h, ϕ_h) solves (2.4).*

Proof. Let $(\sigma_h, \phi_h) \in Z_h \times \Phi_h$ be a solution of (2.4). The definition of Z_h implies the discrete Helmholtz decomposition

$$P_k(\mathcal{T}; \mathbb{R}^2) = Z_h \oplus \operatorname{Curl} Q_h$$

and the sum is orthogonal in $L^2(\Omega)$. Therefore, and because $\Pi_k(\phi_h - \sigma_h) \in P_k(\mathcal{T}; \mathbb{R}^2)$, there exist $\varrho_h \in Z_h$ and $p_h \in Q_h$ such that

$$-\lambda t^{-2} \Pi_k(\phi_h - \sigma_h) = \varrho_h + \operatorname{Curl} p_h. \tag{3.5}$$

The L^2 orthogonality of ϱ_h and $\operatorname{Curl} p_h$ by construction leads to

$$(\varrho_h, \xi_h)_{L^2(\Omega)} = -\lambda t^{-2} (\Pi_k(\phi_h - \sigma_h), \xi_h)_{L^2(\Omega)} \quad \text{for all } \xi_h \in Z_h.$$

Testing (2.4) with $\psi_h = 0$ and $\tau_h = \xi_h$ thus proves (3.4a). Let now $\psi_h \in \Phi_h$. The definition of p_h from (3.5) shows

$$
\begin{aligned}
(\psi_h, \operatorname{Curl} p_h)_{L^2(\Omega)} &= -(\psi_h, \lambda t^{-2} \Pi_k(\phi_h - \sigma_h))_{L^2(\Omega)} - (\psi_h, \varrho_h)_{L^2(\Omega)} \\
&= -(\Pi_k \psi_h, \lambda t^{-2} (\Pi_k \phi_h - \sigma_h))_{L^2(\Omega)} - (\psi_h, \varrho_h)_{L^2(\Omega)}.
\end{aligned}
$$

Testing (2.4) with this ψ_h and $\tau_h = 0$ shows (3.4b). The L^2 orthogonality of σ_h and ϱ_h to $\operatorname{Curl} Q_h$, the definition of p_h, and $\operatorname{Curl} Q_h \subseteq P_k(\mathcal{T}; \mathbb{R}^2)$ prove

$$
\begin{aligned}
&\lambda^{-1} t^2 (\operatorname{Curl} p_h, \operatorname{Curl} q_h)_{L^2(\Omega)} \\
&= (-\Pi_k(\phi_h - \sigma_h) - \lambda^{-1} t^2 \varrho_h, \operatorname{Curl} q_h)_{L^2(\Omega)} = -(\phi_h, \operatorname{Curl} q_h)_{L^2(\Omega)},
\end{aligned}
$$

which is (3.4c). Finally, $Z_h \subseteq P_k(\mathcal{T}; \mathbb{R}^2)$ and (2.4) with $\psi_h = 0$ and τ_h arbitrary proves (3.4d).

Let now $(\varrho_h, \phi_h, p_h, \sigma_h) \in Z_h \times \Phi_h \times Q_h \times Z_h$ be a solution to (3.4). The last equation in (3.4) and $Z_h \subseteq P_k(\mathcal{T}; \mathbb{R}^2)$ show

$$-\lambda t^{-2} (\Pi_k \phi_h - \sigma_h, \tau_h)_{L^2(\Omega)} = (\eta, \tau_h)_{L^2(\Omega)} \quad \text{for all } \tau_h \in Z_h,$$

which is equation (2.4) tested with $\psi_h = 0$. The third equation of (3.4) proves that $\Pi_k \phi_h + \lambda^{-1} t^2 \operatorname{Curl} p_h \in Z_h$. On the other hand, the definition of Z_h and the last and the first equation in (3.4) show for any $\tau_h \in Z_h$

$$
\begin{aligned}
&(\Pi_k \phi_h + \lambda^{-1} t^2 \operatorname{Curl} p_h, \tau_h)_{L^2(\Omega)} = (\phi_h, \tau_h)_{L^2(\Omega)} \\
&= (\sigma_h, \tau_h)_{L^2(\Omega)} - \lambda^{-1} t^2 (\eta, \tau_h)_{L^2(\Omega)} = (\sigma_h - \lambda^{-1} t^2 \varrho_h, \tau_h)_{L^2(\Omega)}.
\end{aligned}
$$

Therefore,

$$\Pi_k \phi_h + \lambda^{-1} t^2 \operatorname{Curl} p_h = \sigma_h - \lambda^{-1} t^2 \varrho_h,$$

which implies the discrete Helmholtz decomposition

$$-\lambda t^{-2} \Pi_k(\phi_h - \sigma_h) = \varrho_h + \operatorname{Curl} p_h.$$

Due to (3.4b), we thus conclude

$$
\begin{aligned}
&a(\phi_h, \psi_h) + \lambda t^{-2} (\Pi_k(\phi_h - \sigma_h), \Pi_k \psi_h)_{L^2(\Omega)} \\
&= a(\phi_h, \psi_h) - (\psi_h, \operatorname{Curl} p_h)_{L^2(\Omega)} - (\varrho_h, \psi_h)_{L^2(\Omega)} = 0,
\end{aligned}
$$

which is (2.4) tested with $\tau_h = 0$. This concludes the proof. $\qquad\square$

We are now in the position to prove an error estimate for the discretisation (2.4) that is robust with respect to the limit $t \to 0$. The error estimate involves the Curl part of the data η, i.e., $\alpha_1 \in H^1(\Omega) \cap L^2_0(\Omega)$ with $\eta = \varrho + \operatorname{Curl} \alpha_1$, which exists because $\eta - \varrho$ is divergence-free. This additional term in the error estimate is due to the non-conformity $Z_h \nsubseteq Z$, see also [14]. Furthermore, the estimate involves the Curl part of the shear force, more precisely $\alpha_2 \in H^1(\Omega) \cap L^2_0(\Omega)$ with $\lambda^{-1} t^2 \eta - (\sigma - \phi) = \operatorname{Curl} \alpha_2$. This again exists, because the left-hand side is divergence-free.

Theorem 3.1 (stability and a priori error estimate). *There exists a unique discrete solution* $(\phi_h, \sigma_h) \in \Phi_h \times Z_h$ *to* (2.4). *Let* $(\phi, \sigma) \in \Phi \times Z$ *be the solution to* (2.1) *and let* ρ, p, ρ_h, p_h *be as in Lemma 3.2. Let furthermore* $\alpha_{1,h}, \alpha_{2,h} \in Q_h$ *be defined through the discrete Helmholtz decompositions of* $\Pi_k \eta$ *and* $\lambda^{-1} t^2 \Pi_k \eta + \Pi_k \phi_h$, *respectively, namely*

$$\operatorname{Curl} \alpha_{1,h} = \Pi_k \eta - \rho_h,$$
$$\operatorname{Curl} \alpha_{2,h} = \lambda^{-1} t^2 \Pi_k \eta + \Pi_k \phi_h - \sigma_h$$

(these functions exists by (2.3) *and* (3.4)*). Then the following error estimate holds*

$$\|D(\phi - \phi_h)\|_{L^2(\Omega)} + \|\sigma - \sigma_h\|_{L^2(\Omega)} + \|p - p_h\|_{L^2(\Omega)} + t\|\operatorname{Curl}(p - p_h)\|_{L^2(\Omega)}$$
$$+ \|\varrho - \varrho_h\|_{L^2(\Omega)} + \|\operatorname{Curl}(\alpha_1 - \alpha_{1,h})\|_{L^2(\Omega)} + \|\operatorname{Curl}(\alpha_2 - \alpha_{2,h})\|_{L^2(\Omega)}$$
$$\lesssim \inf_{\substack{(\psi_h, \tau_h, q_h, \xi_h, \beta_{1,h}, \beta_{2,h}) \\ \in \Phi_h \times X_h \times Q_h \times X_h \times Q_h \times Q_h}} \big(\|D(\phi - \psi_h)\|_{L^2(\Omega)} + \|\sigma - \tau_h\|_{L^2(\Omega)}$$
$$+ \|p - q_h\|_{L^2(\Omega)} + t\|\operatorname{Curl}(p - q_h)\|_{L^2(\Omega)} + \|\varrho - \xi_h\|_{L^2(\Omega)}$$
$$+ \|\operatorname{Curl}(\alpha_1 - \beta_{1,h})\|_{L^2(\Omega)} + \|\operatorname{Curl}(\alpha_2 - \beta_{2,h})\|_{L^2(\Omega)} \big).$$

Proof. The proof employs the equivalence to the mixed system from Lemma 3.2. The definition of Z_h implies that (3.4) is in turn equivalent to the system

$$\begin{pmatrix} -\operatorname{div} \mathbb{C}\varepsilon & -\operatorname{Curl} & -\Pi_{\Phi_h} & 0 & 0 & 0 \\ \operatorname{rot} & \lambda^{-1} t^2 \Delta & 0 & 0 & 0 & 0 \\ -\Pi_k & 0 & 0 & \operatorname{Curl} & \operatorname{id} & 0 \\ 0 & 0 & -\operatorname{rot} & 0 & 0 & 0 \\ 0 & 0 & \operatorname{id} & 0 & 0 & \operatorname{Curl} \\ 0 & 0 & 0 & 0 & -\operatorname{rot} & 0 \end{pmatrix} \begin{pmatrix} \phi_h \\ p_h \\ \varrho_h \\ \alpha_{2,h} \\ \sigma_h \\ \alpha_{1,h} \end{pmatrix} = \begin{pmatrix} 0 \\ 0 \\ \lambda^{-1} t^2 \Pi_k \eta \\ 0 \\ \Pi_k \eta \\ 0 \end{pmatrix},$$

where Π_{Φ_h} denotes the L^2 projection onto Φ_h. The operator Δ is understood as $\Delta : Q_h \to Q_h^*$ and analogously $-\operatorname{div} \mathbb{C}\varepsilon : \Phi_h \to \Phi_h^*$. Note that $\Pi_{\Phi_h} : X_h \to \Phi_h$ and $\Pi_k : \Phi_h \to X_h$ are adjoint operators, and therefore, this defines a symmetric system. Note furthermore that $(\phi, p, \varrho, \alpha_2, \sigma, \alpha_1)$ with α_1, α_2 defined as above is a solution to the corresponding continuous problem.

The spaces Φ_h and X_h are equipped with the norms $\|D \bullet\|_{L^2(\Omega)}$ and $\|\bullet\|_{L^2(\Omega)}$. The variable $p_h \in Q_h$ is measured in the norm $\|\bullet\|_{L^2(\Omega)} + t\|\operatorname{Curl} \bullet\|_{L^2(\Omega)}$ while $\alpha_{1,h}, \alpha_{2,h} \in Q_h$ are measured in $\|\operatorname{Curl} \bullet\|_{L^2(\Omega)}$. The above system satisfies a (continuous and) discrete inf-sup condition with respect to these norms as can be seen recursively: Since $\operatorname{Curl} Q_h \subseteq X_h$, the bilinear form defined by the last line satisfies an inf-sup condition on $(\Phi_h \times Q_h \times X_h \times Q_h \times X_h) \times Q_h$. Furthermore, the kernel is exactly $\Phi_h \times Q_h \times X_h \times Q_h \times Z_h$. Brezzi's splitting lemma [5] implies that it remains to show the inf-sup condition of the remaining saddle-point system on $\Phi_h \times Q_h \times X_h \times Q_h \times Z_h$.

Consider the bilinear form $b : (\Phi_h \times Q_h \times X_h) \times (Q_h \times Z_h)$ defined by

$$b((\psi_h, q_h, \xi_h), (\beta_{2,h}, \tau_h)) := (\xi_h, \operatorname{Curl} \beta_{2,h})_{L^2(\Omega)} + (\xi_h, \tau_h)_{L^2(\Omega)}$$

for all $((\psi_h, q_h, \xi_h), (\beta_{2,h}, \tau_h)) \in (\Phi_h \times Q_h \times X_h) \times (Q_h \times Z_h)$. The choice $\xi_h = \operatorname{Curl} \beta_{2,h} + \tau_h$ shows for $\tau_h \in Z_h$ that

$$b((0, 0, \xi_h), (\beta_{2,h}, \tau_h)) = \|\operatorname{Curl} \beta_{2,h}\|_{L^2(\Omega)}^2 + \|\tau_h\|_{L^2(\Omega)}^2.$$

Hence, b satisfies an inf-sup condition. The kernel of b is $\Phi_h \times Q_h \times \{0\}$. Employing again Brezzi's splitting theorem, we conclude that it remains to show the inf-sup condition for the 3×3 upper left matrix on $\Phi_h \times Q_h \times \{0\}$, which defines a saddle-point system. The projection operator in the third line is now applied to 0 only, and therefore, the corresponding bilinear form trivially satisfies an inf-sup condition with kernel $\Phi_h \times Q_h$. The inf-sup condition of the upper left 2×2 matrix — a perturbed Stokes system — finally follows from the theory of saddle-point systems with penalty term (see, e.g., [6, Section III.4]).

In summary, the complete system satisfies an inf-sup condition. A priori error estimates for the standard theory of saddle point problems (see, e.g., [5]) imply the assertion. $\square$

Remark 3.3. If all of the solution variables are smooth enough, Theorem 3.1 implies the convergence rate

$$\|D(\phi - \phi_h)\|_{L^2(\Omega)} + \|\sigma - \sigma_h\|_{L^2(\Omega)} \leq C(t) h^{k+1}$$

with $h := \max_{T \in \mathcal{T}} h_T$. The constant $C(t)$ is discussed in Remark 3.4.

Remark 3.4. Consider the data η to be chosen in $H^k(\Omega)$ and the exact solution $w \in H^{k+1}(\Omega)$ and $\phi \in H^{k+1}(\Omega; \mathbb{R}^2)$. Then the shear force $\zeta := \lambda t^{-2}(\nabla w - \phi)$ belongs to $H^k(\Omega, \mathbb{R}^2)$ and according to the proof of Lemma 3.2, $\zeta = \varrho + \operatorname{Curl} p$. The field ϱ is the gradient of the solution to the Poisson equation with right-hand side $-\operatorname{div} \zeta$ and p solves the Laplacian with right-hand side $\operatorname{rot} \zeta$ and homogeneous Neumann boundary conditions. The regularity of those two variables therefore also depend on the geometry of Ω. The regularity of α_1 is given by the regularity of η and ϱ by $\operatorname{Curl} \alpha_1 = \eta - \varrho$. Note that, in two dimensions, the operator Curl is equivalent to the gradient. The regularity of α_2 is given by $\operatorname{Curl} \alpha_2 = \lambda^{-1} t^2 \eta - (\sigma - \phi)$. Higher-order Sobolev norms of ϕ and ζ can, however, in general not be estimated uniformly in t [4] so that robust discretizations may require locally refined meshes.

4. Numerical Results

This section provides numerical experiments for the new method with the parameter ℓ chosen as $\ell = \lceil (k+2)/3 \rceil$. The convergence history plots display the relative errors

$$e(\phi) := \frac{\|D(\phi - \phi_h)\|_{L^2(\Omega)}}{\|D\phi\|_{L^2(\Omega)}} \quad \text{and} \quad e(w) := \frac{\|\nabla w - \sigma_h\|_{L^2(\Omega)}}{\|\nabla w\|_{L^2(\Omega)}}$$

in dependence of the mesh size h on uniformly refined meshes for various polynomial degrees k. In all numerical experiments, the material parameters read $\nu = 0.3$, $E = 10^6$, and $\kappa = 5/6$ while various values of t are considered. The test examples are purely artificial smooth functions on square-shaped domains. In this work, we disregard the possibility of local mesh-adaptation due to boundary layers or corner singularities and rather focus on the illustration of convergence

rates and the robustness in the parameter t. The high-order approximation on uniform meshes observed in the numerical tests can, however, not be expected in general due to boundary layers [4].

4.1. Exact smooth solution

In the first numerical example, the domain Ω is the unit square $\Omega = (0,1)^2$ and the exact solution from [10] is given by

$$\phi(x,y) = \begin{bmatrix} y^3(y-1)^3 x^2(x-1)^2(2x-1) \\ x^3(x-1)^3 y^2(y-1)^2(2y-1) \end{bmatrix}$$

and

$$w(x,y) = \frac{1}{3}x^3(x-1)^3 y^3(y-1)^3 - \frac{2t^2}{5(1-\nu)}\Big[y^3(y-1)^3 x(x-1)(5x^2-5x+1)$$
$$+ x^3(x-1)^3 y(y-1)(5y^2-5y+1)\Big].$$

The right-hand side $f(x,y)$ of (1.1) is given by $E/(12(1-\nu^2))$ times

$$\Big[12y(y-1)(5x^2-5x+1)\Big(2y^2(y-1)^2 + x(x-1)(5y^2-5y+1)\Big)$$
$$+ 12x(x-1)(5y^2-5y+1)\Big(2x^2(x-1)^2 + y(y-1)(5x^2-5x+1)\Big)\Big].$$

In this case, the field η with $-\operatorname{div}\eta = f$ is obtained by explicit integration of the polynomial f. Fig. 4.1 displays the convergence history of the relative errors for polynomial degrees $k = 0, 1, 2, 3$ and thickness parameters $t = 1/10$ and $t = 1/100$. As predicted, in this smooth example the convergence rates are optimal in h and the method is robust in t.
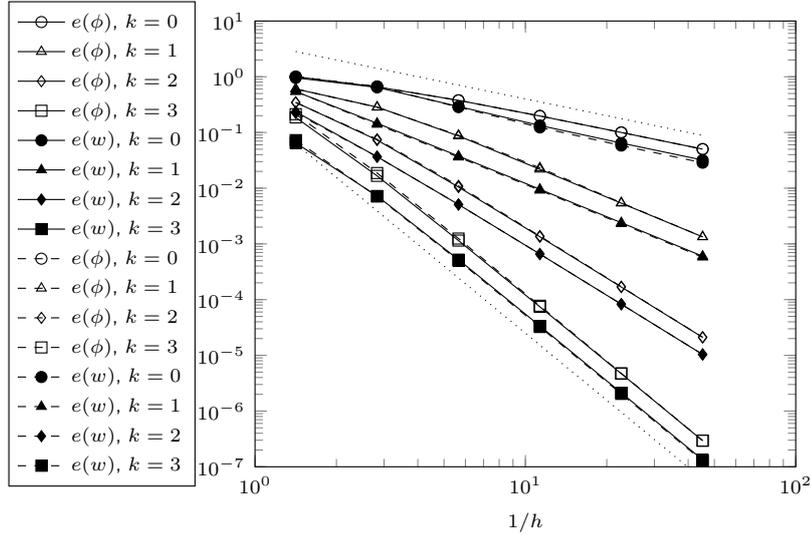

Fig. 4.1. Convergence history for the first numerical experiment for $t = 1/10$ (solid lines) and $t = 1/100$ (dashed lines). The dotted lines without markers indicate the rates $\mathcal{O}(h)$ and $\mathcal{O}(h^4)$.

4.2. Biharmonic equation

The second numerical example is concerned with the solution to the biharmonic equation (Kirchhoff–Love plate). The domain Ω is the square $\Omega = (0, \pi)^2$. The exact solution of the biharmonic equation is given by $w(x, y) = \sin^2(x) \sin^2(y)$, $\phi = \nabla w$, and $f = \frac{E}{12(1-\nu^2)} \Delta^2 w$. The right-hand side η is chosen as $\eta = (-F, 0)$ with the antiderivative F of f with respect to x. While the numerical scheme for the Reissner–Mindlin model will not converge towards this solution, it may be a reasonable approximation as long as t is small compared to h. Fig. 4.2 displays the convergence history for $t = 1/10$, $t = 1/100$, $t = 1/1000$. Pre-asymptotically, optimal-in-h convergence and the robustness with respect to t are observable. The errors are bounded from below by the model error between the two plate models.
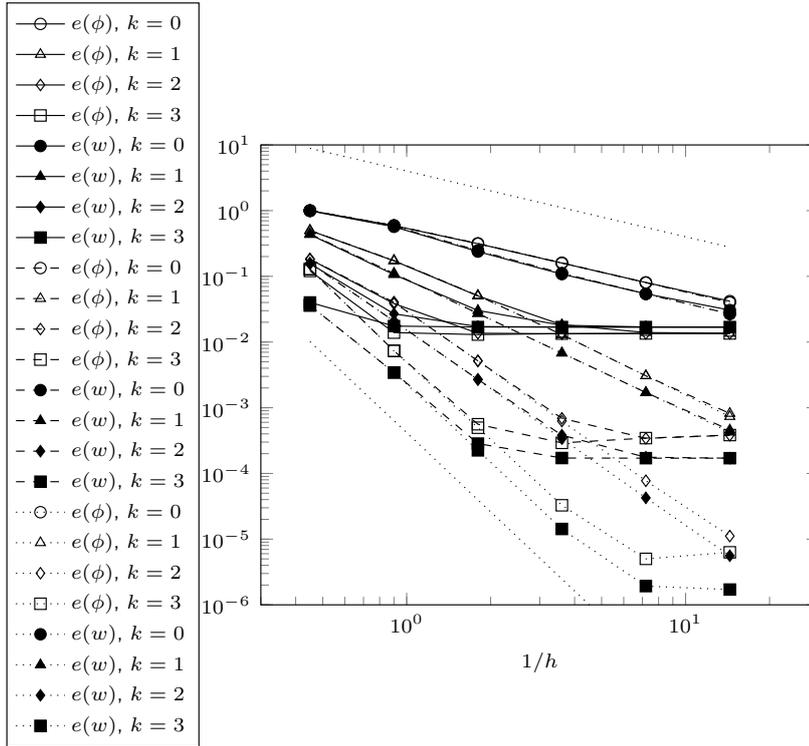

Fig. 4.2. Convergence history for the second numerical experiment for $t = 1/10$ (solid lines), $t = 1/100$ (dashed lines), $t = 1/1000$ (dotted lines). The dotted lines without markers indicate the rates $\mathcal{O}(h)$ and $\mathcal{O}(h^4)$.

References

[1] G. Acosta, R.G. Durán, and M.A. Muschietti, Solutions of the divergence operator on John domains. *Adv. Math.*, **206** (2006), 373–401.

[2] D.N. Arnold, F. Brezzi, and M. Fortin, A stable finite element for the Stokes equations. *Calcolo*, **21** (1984), 337–344.

[3] D.N. Arnold and R.S. Falk, A uniformly accurate finite element method for the Reissner-Mindlin plate. *SIAM J. Numer. Anal.*, **26** (1989), 1276–1290.

[4] D.N. Arnold and R.S. Falk, The boundary layer for the Reissner-Mindlin plate model. *SIAM J. Math. Anal.*, **21** (1990), 281–312.

[5] D. Boffi, F. Brezzi, and M. Fortin, *Mixed finite element methods and applications*, volume 44 of *Springer Series in Computational Mathematics*. Springer, Heidelberg, 2013.

[6] D. Braess. *Finite Elements. Theory, Fast Solvers, and Applications in Elasticity Theory*. Cambridge University Press, Cambridge, third edition, 2007.

[7] S.C. Brenner and L.R. Scott, *The Mathematical Theory of Finite Element Methods*, volume 15 of *Texts in Applied Mathematics*. Springer, New York, third edition, 2008.

[8] F. Brezzi and M. Fortin, Numerical approximation of Mindlin-Reissner plates. *Math. Comp.*, **47** (1986), 151–158.

[9] F. Brezzi, M. Fortin, and R. Stenberg, Error analysis of mixed-interpolated elements for Reissner-Mindlin plates. *Math. Models Methods Appl. Sci.*, **1** (1991), 125–151.

[10] C. Chinosi and C. Lovadina, Numerical analysis of some mixed finite element methods for Reissner–Mindlin plates. *Computational Mechanics*, **16** (1995), 36–44.

[11] P. Clément, Approximation by finite element functions using local regularization. *Rev. Française Automat. Informat. Recherche Operationnelle*, **9** (1975), 77–84.

[12] M. Crouzeix and P.A. Raviart, Conforming and nonconforming finite element methods for solving the stationary Stokes equations. I. *Rev. Française Automat. Informat. Recherche Opérationnelle Sér. Rouge*, **7** (1973), 33–75.

[13] D. Gallistl and M. Schedensack, Taylor–Hood discretization of the Reissner–Mindlin plate. Submitted (2018).

[14] M. Schedensack, A new generalization of the P_1 non-conforming FEM to higher polynomial degrees. *Comput. Methods Appl. Math.*, **17** (2017), 161–185.